JOURNAL OF APPLIED PHYSICS **105**, 073107 (2009)

Electro-optical characteristics of omnidirectional liquid crystal domain mode using doughnut-shaped slit electrodes

Jin Seog Gwag,[1] Kwang-Soo Bae,[2] You-Jin Lee,[2] and Jae-Hoon Kim[2,3,a]
[1]*Department of Physics, Yeungnam University, Gyeongsangbuk–do 712-749, Republic of Korea*
[2]*Department of Information Display Engineering, Hanyang University, Seoul 133-791, Republic of Korea and Department of Electronics and Computer Engineering, Hanyang University, Seoul 133-791, Republic of Korea*
[3]*Research Institute of Information Display, Hanyang University, Seoul 133-791, Republic of Korea*

(Received 11 September 2008; accepted 18 December 2008; published online 10 April 2009)

This paper proposes a liquid crystal (LC) display (LCD) mode, characterized by an azimuthally continuous nematic domain, driven by patterned electrodes with circular- and doughnut-shaped slits producing conelike fields, as a vertically aligned (VA) nematic LC mode. This proposed mode is focused on achieving a high transmittance display with omnidirectionally uniform optical characteristics by utilizing the proposed electrode structure. Consequently, the experimental results of the proposed LCD mode show high brightness and wide viewing angles that correlate well to numerical calculations. Other electro-optics characteristics of this mode correspond to the patterned VA LC mode. © *2009 American Institute of Physics*. [DOI: 10.1063/1.3075593]

I. INTRODUCTION

Liquid crystal (LC) displays (LCDs) control their gray levels by electrically modulating the optical anisotropy of the LC, determining the polarization of the light. Improved controllability of the electro-optical characteristics in LCD technologies, such as contrast ratio, response time, and viewing angle, has enabled thin-film transistor LCDs to rapidly expand in the display market. Recently, high efficient LCDs, with high aperture ratios, are becoming more interesting as they can achieve more vivid images, as well as having lower power consumption thus saving energy.

Several types of LCD modes,[1–15] which are determined by the initial LC configuration and electrode structure, have been proposed, including twisted nematic (TN), in-plane switching (IPS), and vertically aligned (VA) modes. The TN mode has been most widely used in mass production of LCDs due to its high transmittance and simple fabrication process; however it does not give an effective image at the wider side viewing angles. Therefore, advanced LC modes,[1–4] free from this drawback, have been developed competitively, such as IPS and VA modes which show far better electro-optical viewing characteristics.

The IPS mode has good viewing angle characteristics without the need for any compensation film because the effective retardation of the LC layer at the *off* axis is similar to that at the *on* axis. The IPS mode also displays uniform gray levels and colors but it has relatively low transmittance compared to the TN mode since the LCs are almost VA on the electrode due to the direction of the electric field.

As a competitor of the IPS mode, VA nematic modes with multidomain LC structure have been attractive in LC displays because of their high contrast ratios. The patterned VA (PVA) mode is one such representative VA mode and it is characterized by its chevron-shaped electrode to induce four domain-LC structures for producing practical wide viewing angles by adopting compensation films and having very high contrast ratios resulting from its excellent dark state. Nevertheless, in a more desirable case, the LCD should show uniform electro-optic characteristics at all viewing angle directions, which could be achieved by the LC cell having azimuthally omnidirectional LC direction distribution, otherwise known as a real multidomain structure. Therefore, it is crucial to design a new type of electrode to create an advanced LCD to drive this type of wide angle viewing directional capability. This paper presents an omnidirectional LC domain (OLD) mode characterized by a conelike field induced from patterned electrodes with circular- and doughnut-shaped slits.

II. OPTICAL PRINCIPLE

Figure 1(a) shows the cross sectional structure of the proposed OLD cell. The optical structure of this mode consists of the top polarizer and a $\lambda/4$ retardation film with an optical axis of 135° with respect to the optical axis of the bottom polarizer on the top substrate and a $\lambda/4$ retardation film with an optical axis of 45° and the bottom polarizer under the bottom substrate. Moreover, the A plate and positive or negative C plates are added to compensate for the optical mismatch for the side viewing situations. Figure 1(b) shows the structure of the top and bottom electrodes from the top view. In order to achieve a conelike electric field in the cell, the hole in the circular type electrode and the doughnut-shaped slit structure are formed in the top and the bottom electrodes, respectively. Consequently, the LCs will fall down to the azimuthally omnidirection by the field direction caused from the electrode structure, as shown in Fig. 1(c). To describe the optically dark and bright states of this directional configuration, the polarization path of the light on the Poincare sphere, when the incident light passes through each layer, was used as a simple optical principle of the OLD

---

[a]Electronic mail: jhoon@hanyang.ac.kr.

© 2009 American Institute of Physics

Downloaded 03 Jul 2010 to 166.104.145.57. Redistribution subject to AIP license or copyright; see http://jap.aip.org/jap/copyright.jsp

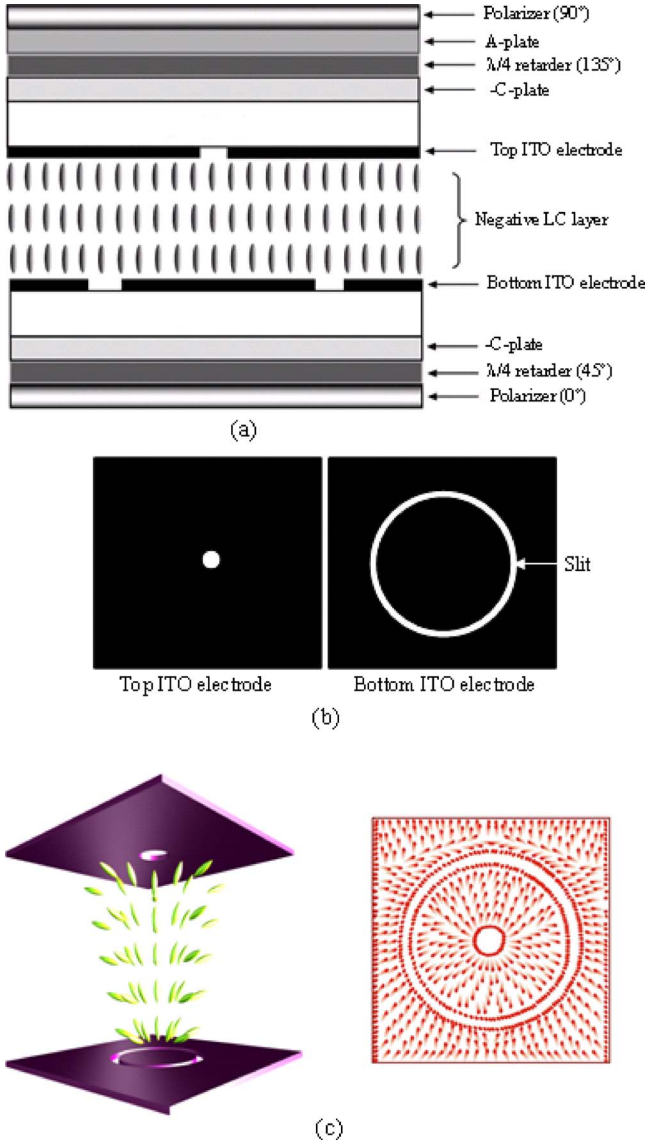

FIG. 1. (Color online) Schematic diagram in the OLD mode: (a) cross-sectional structure of the OLD mode. (b) The structure of the top and bottom electrodes (top view). (c) LC behavior under applied voltage field on state (side and top views).

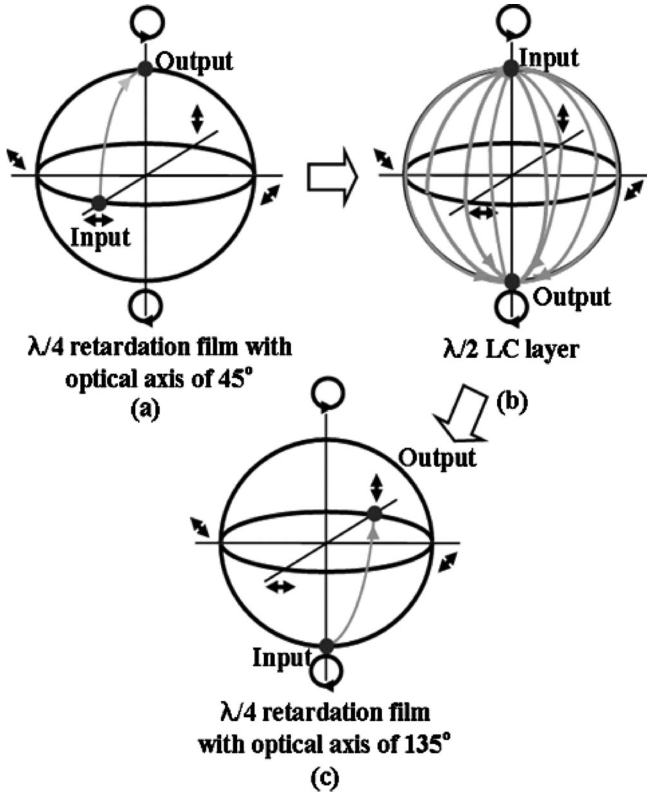

FIG. 2. Poincare sphere representation of the optical principle of the OLD mode: (a) the path of light passing through the λ/4 retardation film at an optical axis of 45°. (b) The path of light passing through the λ/2 LC layer. (c) The path of light passing through the λ/4 retardation film at an optical axis of 135°.

mode, as shown in Fig. 2. In the initial state, with VA LCs, the linearly polarized light to the 0° direction by the bottom polarizer becomes the left-handed circular polarization state after passing through the λ/4 retardation film with an optical axis of 45°, as shown in Fig. 2(a). In the next step, passing through the LC layer, the polarization of the light is not changed due to homeotropic LC alignment without the optical phase retardation; therefore the light maintains the circular polarization state. In the final step, passing through the λ/4 retardation film with an optical axis of 135°, the polarization state of the light returns to its original state, namely, 0° polarization. Therefore, good darkness can be obtained at the VA initial LC state. On the other hand, when a voltage was applied to the electrode, the left-handed circular polarized light, after passing through the λ/4 retardation film with optical axis of 45°, is divided into various polarization paths at each domain when passing the LC layer with an optical phase retardation of λ/2, as shown in Fig. 2(b). However, ultimately all the lights are placed on the south pole of the Poincare sphere, being the right-handed circular polarization after passing the LC layer. Finally, after passing through the λ/4 retardation film with an optical axis of 135°, the light is linearly polarized to the 90° direction, as shown in Fig. 2(c). Therefore, the maximum brightness can be obtained under the electric field that produces the effective retardation of λ/2 at the LC layer. Results, calculated by the 2×2 Jones matrix,[16,17] also establish an obviously bright state of this optical configuration. Jones matrix of a phase retardation film can be expressed as

$$J_{\text{film}} = e^{i(\pi d/\lambda)}(n_e' + n_o)\begin{bmatrix} a & b \\ -b^* & a^* \end{bmatrix}.$$

Here,

$$a = \frac{1}{\sqrt{1+u^2}}\sin\phi\,\sin(\sqrt{1+u^2}\phi) + \cos\phi\,\cos(\sqrt{1+u^2}\phi) + i\frac{u}{\sqrt{1+u^2}}\cos\phi\,\sin(\sqrt{1+u^2}\phi),$$

$$b = \frac{1}{\sqrt{1+u^2}}\cos\phi\,\sin(\sqrt{1+u^2}\phi) - \sin\phi\,\cos(\sqrt{1+u^2}\phi) + i\frac{u}{\sqrt{1+u^2}}\sin\phi\,\sin(\sqrt{1+u^2}\phi),$$

where ϕ is the twisted angle of LC ($\phi=0$ in the proposed mode) and

Downloaded 03 Jul 2010 to 166.104.145.57. Redistribution subject to AIP license or copyright; see http://jap.aip.org/jap/copyright.jsp

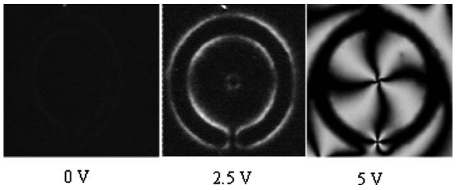

FIG. 3. Microscopic images showing the LC distribution due to an electric field applied to the proposed doughnut-shaped slitted electrode.

$$u = \frac{\pi d}{\lambda \phi}\left(\frac{1}{d}\int_0^d \frac{n_e n_o}{\sqrt{n_e^2 \sin^2\theta + n_o^2\cos^2\theta}}dz - n_o\right).$$

Here d, λ, n_e, n_o, and θ are the cell gap, the wavelength of light, the extraordinary refractive index, the ordinary refractive index, and the pretilt angle of LC, respectively. Subsequently, we calculate transmittance in the optical configuration of OLD mode as follows:

$$E = \begin{bmatrix} 0 \\ 1 \end{bmatrix}\begin{bmatrix} \cos 135° & -\sin 135° \\ \sin 135° & \cos 135° \end{bmatrix}\begin{bmatrix} a_3 & b_3 \\ -b_3^* & a_3^* \end{bmatrix}$$

$$\times \begin{bmatrix} \cos 135° & \sin 135° \\ -\sin 135° & \cos 135° \end{bmatrix}\begin{bmatrix} \cos\beta & -\sin\beta \\ \sin\beta & \cos\beta \end{bmatrix}$$

$$\times \begin{bmatrix} a_2 & b_2 \\ -b_2^* & a_2^* \end{bmatrix}\begin{bmatrix} \cos\beta & \sin\beta \\ -\sin\beta & \cos\beta \end{bmatrix}$$

$$\times \begin{bmatrix} \cos 45° & -\sin 45° \\ \sin 45° & \cos 45° \end{bmatrix}\begin{bmatrix} a_1 & b_1 \\ -b_1^* & a_1^* \end{bmatrix}$$

$$\times \begin{bmatrix} \cos\alpha_1 & \sin 45° \\ -\sin\alpha_1 & \cos 45° \end{bmatrix}\begin{bmatrix} 1 \\ 0 \end{bmatrix}.$$

Then, the transmittance is given by

$$T = |\mathrm{Re}[E]|^2 + |\mathrm{Im}[E]|^2 = (\sin^2\beta + \cos^2\beta)^2 = 1. \quad (1)$$

Here, β is the optical axis of the LC and Eq. (1) indicates that the transmittance in this optical configuration is not dependent on orientation of any preferred LC directional characteristic but is the same for all orientations. This is the reason why the optical transmittance of the OLD mode is higher.

III. EXPERIMENTAL RESULTS

To check whether this electrode structure actually produces azimuthally omnidirectional distribution of the LC directors under an electric field or not, microscopic images of the LC cells are examined with a crossed polarizer without the λ/4 film. Figure 3 shows the optical images of the LC cell under 0, 3, and 5 V. As expected, the image at 5 V clearly indicates that the LC directors are distributed through a radial shape with respect to the central hole in the top electrode.

In order to study the optical characteristics of the OLD and the PVA modes, simulations were carried out on the basis of the 2×2 extended Jones matrix method[18] as a preferred optical calculation method using commercial LCD simulations supported by TechWiz LCD. Figure 4(a) shows the transmittance as a function of the applied voltage of the OLD and the PVA modes with vertical switching. As the cell conditions lead to the simulation results, two polarizers are set to be crossed with each other and the cell gap is 3.5 μm. The dielectric anisotropy and birefringence of the LC were $\Delta\varepsilon = -3$ and $\Delta n = 0.1$, respectively. In case of OLD mode, the hole size in the top electrode was 10 μm. The diameter of the ring slit and its width in the bottom electrode were 100 and 20 μm, respectively. It is known that the threshold voltage is approximately 2 V, and the driving voltage is below 6 V. In case of PVA mode, slit and electrode widths were 10 and 70 μm, respectively. It is known that the threshold voltage is approximately 2 V, and the driving voltage is over 6 V. Above all things, simulated results in Fig. 4(a) show obviously that the transmittance of the OLD mode is higher than that of the PVA mode with electrode structure of chevron shape.

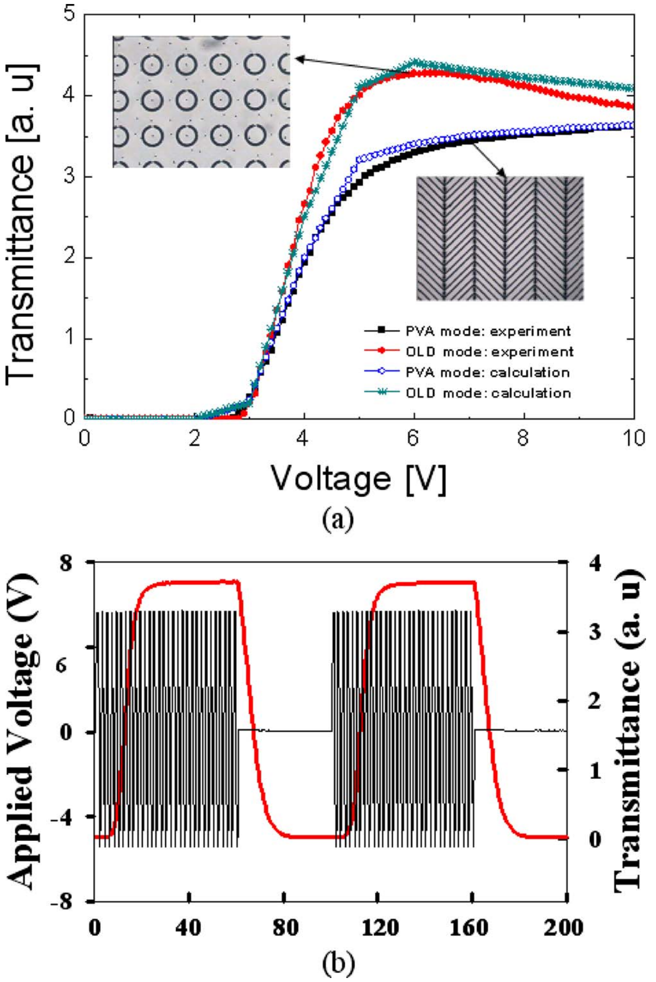

FIG. 4. (Color online) (a) The simulated and measured optical transmittance curves as a function of electric field for the OLD and the PVA modes. The inset photograph images show the bright states of the fabricated samples. (b) Response time of the OLD cell.

In order to confirm the simulated results, we prepared PVA and OLD cells with cell gap of 3.7 μm. In the fabricated cell conditions of the OLD mode, the hole size in the top electrode, slit diameter, and width in the bottom electrode agree with the simulation conditions presented above. The LC (MLC 6610, Merck) with a negative dielectric anisotropic ($\Delta\varepsilon = -3.1$ and $\Delta n = 0.099$) was used in this experiment and AL1H659 (JSR Corp., Japan) was used as the material to

Downloaded 03 Jul 2010 to 166.104.145.57. Redistribution subject to AIP license or copyright; see http://jap.aip.org/jap/copyright.jsp

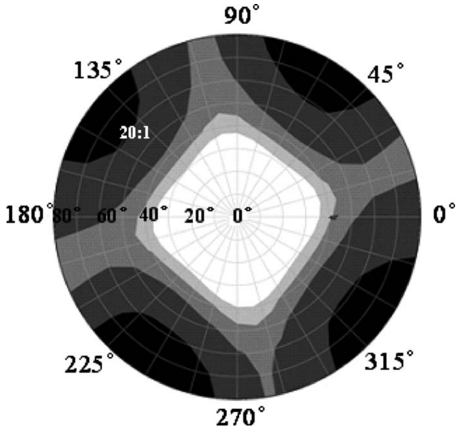

FIG. 5. Calculated viewing angle characteristics of the OLD mode using compensation films (A plate and negative C plate).

align the LC to the vertical direction in the initial state. A 1 kHz square-wave voltage was applied to the electrode for horizontal switching, a halogen lamp was used as a light source, and a signal function generator (DS345 of Stanford Research Systems) was used as a voltage source. Figure 4(a) shows also the measured electro-optic characteristics and photograph images taken at the bright states of the OLD and the PVA cells, with uniform LC alignment. The experimental results correlate well with the numerical calculations, as shown in Fig. 4(a). As expected at simulated results of the figure, the OLD mode shows 20% higher brightness than the PVA mode. The response time of the OLD is shown in Fig. 4(b). The rise and decay times were measured at 10 and 16 ms at room temperature, respectively, similar to the PVA mode. If the diameter of the ring-shaped slit is shortened, the response speed will become faster. Figure 5 shows the calculated viewing angle of the OLD mode with the compensation films of negative C and A plates. A contrast ratio greater than 10:1 can be achieved from almost all viewing areas in the contours having polar angle limits of ±80°. On the basis of these electro-optical characteristics, it can be seen that the OLD mode is sufficient for various LCD applications and can achieve high efficiencies.

IV. CONCLUSION

A highly efficient LCD mode is proposed, having an azimuthally continuous nematic domain, driven by a cone-like field produced by a circular type slitted electrode. The proposed LCD mode can obtain high transmittance and as a result of the experimental studies presented, the proposed LCD mode, with $\lambda/4$ film, shows high brightness under wide viewing angles, and its electric-optic characteristics correlate well with numerical calculations. The response time of this mode corresponds to the PVA mode and it is expected that this LCD mode will be used in various LC applications requiring vivid images as well as low power consumption.

ACKNOWLEDGMENTS

This work was supported by Samsung Electronics Co., Ltd. and the Korea Research Foundation Grant funded by the Korean Government (MOEHRD)" (Grant No. KRF-2006-005-J04103).

[1] T. Miyashita, Y. Yamaguchi, and T. Uchida, Jpn. J. Appl. Phys., Part 2 **34**, L177 (1995).
[2] K. H. Kim, K. Lee, S. B. Park, J. K. Song, S. N. Kim, and J. H. Souk, *The 18th International Display Research Conference Asia Display '98* (Society for Information Display, Seoul, 1998), p. 383.
[3] M. Oh-e and K. Kondo, Appl. Phys. Lett. **67**, 3895 (1995).
[4] S. H. Lee, S. L. Lee, and H. Y. Kim, Appl. Phys. Lett. **73**, 2881 (1998).
[5] P. J. Bos and K. R. Koehler-Beran, Mol. Cryst. Liq. Cryst. **113**, 329 (1984).
[6] J. S. Gwag, K.-H. Park, J. L. Lee, J. C. Kim, and T.-H. Yoon, Jpn. J. Appl. Phys., Part 1 **44**, 1875 (2005).
[7] J. S. Gwag, Y.-J. Lee, M.-E. Kim, J.-H. Kim, J. C. Kim, and T.-H. Yoon, Opt. Express **16**, 2663 (2008).
[8] J. S. Gwag, K. Sohn, Y.-K. Kim, and J.-H. Kim, Opt. Express **16**, 12220 (2008).
[9] J. S. Gwag, Y.-J. Lee, J.-H. Kim, H. J. Lee, and M. H. Yi, Opt. Express **16**, 18102 (2008)..
[10] D.-K. Yang, J. L. West, L. C. Chien, and J. W. Doane, J. Appl. Phys. **76**, 1331 (1994).
[11] N. A. Clark and S. T. Lagerwall, Appl. Phys. Lett. **36**, 899 (1980).
[12] D. W. Berreman and W. R. Heffner, Appl. Phys. Lett. **37**, 109 (1980).
[13] J. S. Gwag, J. Fukuda, M. Yoneya, and H. Yokoyama, Appl. Phys. Lett. **91**, 073504 (2007).
[14] J. S. Gwag, J.-H. Kim, M. Yoneya, and H. Yokoyama, Appl. Phys. Lett. **92**, 153110 (2008).
[15] J. S. Gwag, M. Oh-e, K.-R. Kim, S.-H. Cho, M. Yoneya, H. Yokoyama, H. Satou, and S. Itami, Nanotechnology **19**, 395301 (2008).
[16] R. C. Jones, J. Opt. Soc. Am. **32**, 486 (1942).
[17] H. L. Ong, J. Appl. Phys. **64**, 614 (1988).
[18] A. Lien, Appl. Phys. Lett. **57**, 2767 (1990).

Downloaded 03 Jul 2010 to 166.104.145.57. Redistribution subject to AIP license or copyright; see http://jap.aip.org/jap/copyright.jsp